The EMBO Journal vol.14 no.17 pp.4123–4131, 1995

Solution structure of porcine pancreatic phospholipase A_2

Bert van den Berg, Marco Tessari[1], Gerard H.de Haas, Hubertus M.Verheij, Rolf Boelens[1] and Robert Kaptein[1,2]

Center for Biomembranes and Lipid Enzymology, Division of Enzymology and Protein Engineering, and [1]Bijvoet Center for Biomolecular Research, Utrecht University, Padualaan 8, 3584 CH Utrecht, The Netherlands

[2]Corresponding author

The lipolytic enzyme phospholipase A_2 (PLA_2) is involved in the degradation of high-molecular weight phospholipid aggregates *in vivo*. The enzyme has very high catalytic activities on aggregated substrates compared with monomeric substrates, a phenomenon called interfacial activation. Crystal structures of PLA_2s in the absence and presence of inhibitors are identical, from which it has been concluded that enzymatic conformational changes do not play a role in the mechanism of interfacial activation. The high-resolution NMR structure of porcine pancreatic PLA_2 free in solution was determined with heteronuclear multidimensional NMR methodology using doubly labeled ^{13}C,^{15}N-labeled protein. The solution structure of PLA_2 shows important deviations from the crystal structure. In the NMR structure the Ala1 α-amino group is disordered and the hydrogen bonding network involving the N-terminus and the active site is incomplete. The disorder observed for the N-terminal region of PLA_2 in the solution structure could be related to the low activity of the enzyme towards monomeric substrates. The NMR structure of PLA_2 suggests, in contrast to the crystallographic work, that conformational changes do play a role in the interfacial activation of this enzyme.

Keywords: doubly labeled protein/interfacial activation/phospholipase A_2/solution structure

Introduction

Phospholipases A_2 (PLA_2s; EC 3.1.1.4) are calcium-dependent lipolytic enzymes that stereospecifically cleave the *sn*-2 acyl linkage of *sn*-3-phospholipids (Waite, 1987). They occur widespread in nature and are small homologous proteins consisting of 120–125 amino acids. PLA_2s are very stable under denaturing conditions, because of the presence of six or seven disulfide bridges. Over 90 primary structures have been determined, and the crystal structures of several PLA_2s have been solved. Among them are the enzymes from bovine and porcine pancreas (Dijkstra *et al.*, 1981, 1982, 1983), several snake venom PLA_2s (Brunie *et al.*, 1985; Scott *et al.*, 1990; Westerlund *et al.*, 1992) and the human synovial fluid (human platelet) PLA_2 (Wery *et al.*, 1991). All these enzymes show a remarkable similarity in their three-dimensional structures. A mechanism of catalysis has been proposed, based on crystallographic and biochemical data (Verheij *et al.*, 1980).

Pancreatic phospholipases have a low catalytic activity towards monomeric substrates. When phospholipid substrates are present in an aggregated state like micelles, the enzymes become two to three orders of magnitude more active. This phenomenon of enzymatic activation at lipid–water interfaces is called interfacial activation and is one of the central themes in lipolysis. Several models have been suggested to explain the activation process (Volwerk and de Haas, 1982; Scott *et al.*, 1990). These models can be classified in two groups, the substrate models and the enzyme models. The substrate models attribute the high activity of the PLA_2 in the presence of interfaces to the altered properties of the substrate in these interfaces. One important substrate model assumes that the phospholipids in the aggregate have a conformation which makes a facilitated diffusion into the active site possible (Scott *et al.*, 1990; Scott and Sigler, 1994). A common feature of all substrate models is that the enzyme is thought to be structurally invariant, irrespective of the absence or presence of a lipid–water interface. In contrast, in the enzyme models it is the enzyme itself that is thought to become activated. Binding of the enzyme to the interface would result in a conformational change in the enzyme, leading to a more efficient catalysis of substrates (Verger and de Haas, 1976).

The interfacial activation of PLA_2 has been addressed by several biochemical and X-ray studies of PLA_2s complexed to monomeric inhibitors (Thunnissen *et al.*, 1990; White *et al.*, 1990; Scott *et al.*, 1991; Tomoo *et al.*, 1992). In most cases very similar structures for the free and inhibited enzymes were observed, leading to the conclusion that no major structural changes occur upon binding of monomeric and aggregated lipids in the active site of the enzyme. An entirely different situation is encountered for lipases. X-ray structures, which were recently determined for two lipases, show that large structural changes are induced when these lipolytic enzymes bind a monomeric inhibitor in the active site (Brady *et al.*, 1990; Brzozowski *et al.*, 1991) or when the enzyme binds to lipid micelles (Tilbeurgh *et al.*, 1993).

In order to investigate further the mechanism of interfacial activation we set out to determine the nuclear magnetic resonance (NMR) structures of free PLA_2 and that of the enzyme complexed to lipid micelles. Due to the small size of PLA_2, NMR spectroscopy is an attractive method to determine the structure of PLA_2 complexed to micelles. As a start NMR studies were performed on free porcine pancreatic PLA_2, because the structure of the free enzyme can serve as a reference to locate structural changes when the enzyme binds to the micelles. With multidimensional NMR techniques the assignment of the

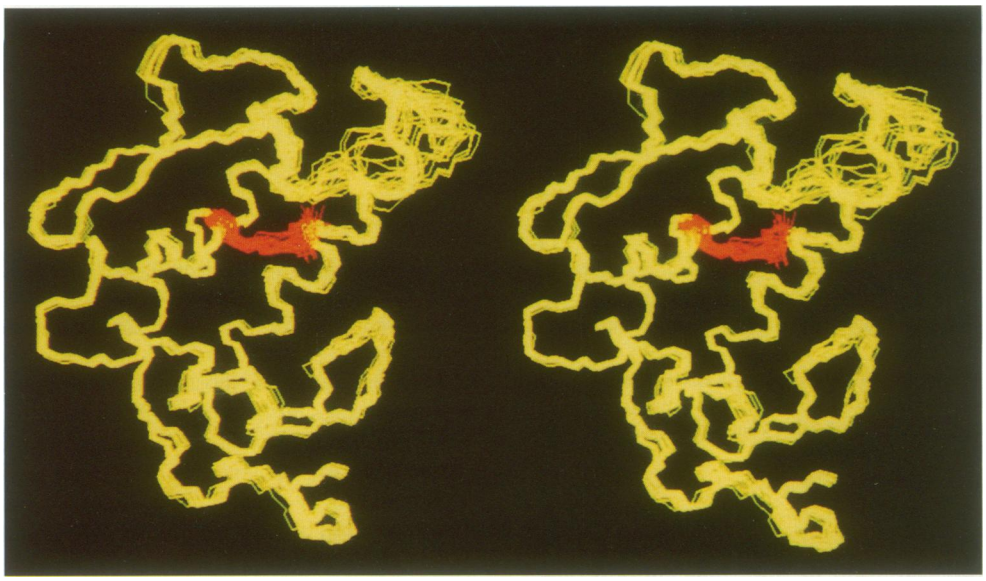

Fig. 1. Stereoviews showing best-fit superpositions of the backbone (N, C_α, C′) atoms of the final 20 refined distance geometry structures of free PLA_2. The backbones of the first four N-terminal residues (Ala1, Leu2, Trp3 and Gln4) are shown in red.

^1H and ^{15}N resonances was largely completed and a secondary structure was determined (Fisher *et al.*, 1989; Dekker *et al.*, 1991). Recently it was shown that high-resolution NMR structures can be obtained from assignment of a large number of nuclear Overhauser effects (NOEs) between amino acid side chains, using ^{13}C-edited NOESY experiments to solve overlap in the aliphatic regions of the NMR spectra (Clore and Gronenburg, 1991; Clore *et al.*, 1993). In the present study, using doubly labeled [^{13}C,^{15}N]PLA_2, we describe the determination of the three-dimensional NMR structure of free porcine pancreatic PLA_2. When comparing this structure with the crystal structure it appears that there exist important structural differences, which support models involving enzymatic structural changes in the interfacial activation of PLA_2.

Results and discussion

Resonance and NOE assignments of PLA_2

The backbone resonances of PLA_2 were assigned using three-dimensional (3D) HNCO, HNCA, HNCOCA and HCACO triple-resonance experiments, in combination with the 3D ^{15}N-edited TOCSY-HSQC experiment. The only backbone NH resonance which is missing in the assignment is the Ala1 α-amino group, presumably due to exchange with the solvent (Peters *et al.*, 1992). The triple-resonance approach made it possible to confirm and extend the sequential assignments made by Dekker *et al.* (1991), who used the conventional assignment approach using sequential NOEs (Wüthrich, 1986). Starting from the Hα and the Cα resonances, the assignment of the amino acid side chains in most cases was straightforward, using the HCCH-COSY and several HCCH-TOCSY experiments. At the end of the procedure, >98% of the side chain ^1H and ^{13}C resonances were assigned (the assignments, as well as the constraint list and the co-ordinates of the structures have been deposited at the Brookhaven Protein Databank). The assignments for the aromatic side chains were obtained from 2D TOCSY spectra, and from the observation of intra-residue NOEs from aromatic ring protons to the CαH and CβH protons in a 3D ^{13}C-edited NOESY spectrum. The stereospecific assignments of the prochiral methyl groups of the leucine and valine residues was easily accomplished by analysis of a ^1H-^{13}C HMQC spectrum of a 10% ^{13}C-labeled PLA_2 sample (Senn *et al.*, 1989). The recording and analysis of ^{13}C-edited NOESY spectra was crucial to obtain a large number of long range contacts between aliphatic amino acid side chains. The quality of the ^{13}C-edited NOESY spectra was sufficient to obtain more than 1700 distance constraints, comprising 549 long range contacts.

The final structures

A total of 35 distance geometry (DG) structures was calculated. The DG structures do not contain calcium, because no experimental NMR constraints are available for this ion. However, during the refinement stage it was found necessary to constrain the calcium ion in order to maintain the DG conformation of the calcium binding loop. Without constraints for calcium the loop appeared to drift away during molecular dynamics calculations. Similar behaviour was found in a molecular dynamics study carried out by Demaret and Brunie (1990), who removed the calcium ion prior to the calculations. According to these authors the results were 'a disaster', as this approach gave molecules that were flattened out.

After inspection of the 35 distance geometry structures for chirality, distance and dihedral angle violations, 33 structures were refined. None of these structures displayed distance violations larger than 0.7 Å or φ angle violations larger than 20°. After analysis for low total energies and violation energies a final set of 20 refined structures was obtained. The superposition of the backbone (N, C_α, C′) atoms of these 20 structures is shown in Figure 1. The precision of the current structure is indicated in Figure 2, where the r.m.s. differences of the 20 conformers with respect to the mean coordinate positions are shown as a

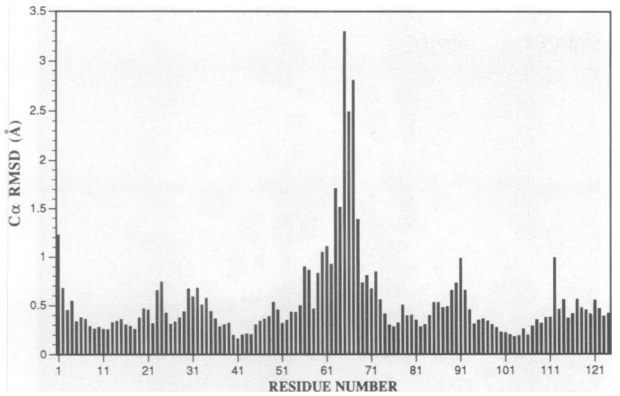

Fig. 2. Atomic r.m.s. distribution (in Å) for the α-carbon atoms of the 20 refined distance geometry structures of PLA_2 about the mean distance geometry structure, as a function of the residue number.

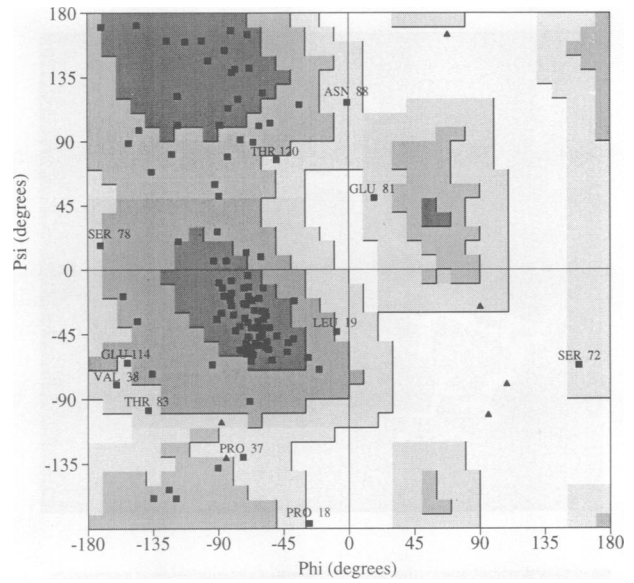

Fig. 3. Ramachandran ϕ/ψ plot for the restrained minimized averaged NMR structure of PLA_2. Non-glycine residues present within the generously allowed regions of the Ramachandran plot are labeled. The core region, allowed region, generously allowed region, and the disallowed region of the plot are coloured black, dark grey, grey, and white, respectively. The plot was generated using the program PROCHECK (Morris *et al.*, 1992).

function of the residue number. It is clear that the structure is well-defined, with the exceptions of the first N-terminal residues and the surface loop running from residue 62 to 72, which are disordered. The r.m.s. difference between the 20 conformers and the averaged structure is 0.68 ± 0.08 Å for the backbone (N, C_α, C′) atoms and 1.08 ± 0.07 Å for all atoms. If the disordered surface loop (residues 62–72) is not taken into account, these r.m.s. difference values drop to 0.47 ± 0.06 Å for the backbone atoms and 0.87 ± 0.05 Å for all atoms. The 20 conformers show on average two distance constraint violations larger than 0.5 Å (the largest violation was 0.65 Å) and seven ϕ angle torsion constraints larger than 5° (largest violation 20°).

The stereochemical quality of the 20 conformers was checked with the program PROCHECK (Morris *et al.*, 1992). All 20 structures, as well as the energy minimized averaged structure, have reasonable to good stereochemical

Table I. Summary of the secondary structure elements present in the NMR structure of porcine pancreatic PLA_2, together with the secondary structure elements in the crystal structures of PLA_2 determined by Dijkstra *et al.* (1983) and Finzel *et al.* (1991)

Secondary structure elements	NMR	X-ray (Finzel)	X-ray (Dijkstra)
Helices			
A	4–13	1–13	1–13
B	18–23	17–22	17–22
C	40–58	39–57	39–57
D	–	–	67–71
E	90–109	89–108	89–108
β-strands			
A	74–78	75–78	74–78
B	81–85	81–84	81–85
Turns			
A	13–16	13–16	13–16
B	–	58–61	–
C	–	63–66	–
D	–	64–67	–
E	–	67–70	67–70
F	–	68–71	68–71
G	78–81	78–81	78–81
H	85–88	85–88	85–88
I	–	112–115	112–115
J	113–116	113–116	113–116
K	114–118	–	–
L	–	119–122	120–124

qualities. The Ramachandran plot of the restrained minimized averaged structure is shown in Figure 3. Approximately 70% of the backbone torsion angles fall within the core regions of the Ramachandran plot (classification 2). The residues found in the generously allowed regions are located in surface loops and turns. No backbone torsion angles other than for proline and glycine residues are present within the disallowed regions of the Ramachandran plot.

From Figure 2 it can be seen that the largest r.m.s. deviations occur for Ala1 and especially for the residues in the surface loop running from residue 62 to 72. With the exception of the aromatic residues Phe63 and Tyr69, only a few long range contacts from the surface loop to the rest of the protein can be found. A possible reason for the low number of NOEs is that this part of the protein is flexible in solution, which is supported by the high intensity of cross peaks of resonances of the surface loop in the TOCSY spectra.

Description of the structure

Due to the presence of seven disulfide bridges the overall structure of PLA_2 is very compact. The molecule contains four α-helices and one antiparallel β-sheet, which consists of two short β-strands connected by a turn. Furthermore, several β-turns and two large surface loops are present. The secondary structure elements present in the (averaged minimized) NMR structure and in both X-ray structures (Dijkstra *et al.*, 1983; Finzel *et al.*, 1991) are summarized in Table I. It is evident that the secondary structure is very similar in the NMR and X-ray structures. The most notable exception is the N-terminal helix A, which is disordered in solution from Ala1 to Trp3. We note that

Table II. Amide ^{15}N and ^{1}H chemical shifts (in p.p.m.) of the N-terminal peptide region of free PLA_2, and of the enzyme in the complex with micelles and inhibitor

	PLA_2 pH 4.3		PLA_2 pH 6.9		Ternary complex pH 4.3	
	(^{15}N,	^{1}H)	(^{15}N,	^{1}H)	(^{15}N,	^{1}H)
L2	125.0	8.97	123.6	9.03	121.0	8.83
W3	115.9	8.03	115.8	8.09	112.6	6.95
Q4	122.8	6.72	123.1	6.81	123.5	6.43
F5	121.5	7.54	121.9	7.50	121.3	7.67
R6	115.9	8.03	115.8	8.09	116.8	7.89
S7	115.2	7.53	114.8	7.55	115.2	7.28
M8	124.7	8.61	125.1	8.61	125.1	8.84

this disorder in the N-terminal region is real since NOEs linking this region with the protein core are genuinely absent. In contrast, a large number of NOEs indicating a well-defined α-helical conformation of the N-terminus were observed in the spectra of an enzyme–inhibitor complex bound to lipid micelles (van den Berg *et al.*, 1995). It might be argued that the differences we observed are due to the low pH of 4.3 at which the solution structures were determined. At this pH the histidines and acidic residues can be expected to be at least partially protonated. However, it appears that this only affects the structure of the loop regions, but not that of the core of the protein (apart from the N-terminal helix). We have recently shown that the activity of the enzyme at pH 5.0 and 4.0 is 55 and 10%, respectively, of the optimum value at pH 6 (S.W.J.Beiboer, B.van den Berg, N.Dekker, R.C.Cox and H.M.Verheij, manuscript in preparation). Also, a comparison of the crystal structure of a snake venom PLA_2, determined at pH 4.2 in the absence of calcium, with that of bovine pancreatic PLA_2, determined at pH 7.6 in the presence of calcium, showed that 'the homologous core structure has a nearly superimposable backbone' (Renetseder *et al.*, 1985).

An important part of our arguments rests on the conformation of the N-terminal peptide region (Ala1–Leu2–Trp3), which in all crystal structures is in an α-helical conformation with the α-amino group in a buried and hydrogen-bonded position. In ^{15}N-^{1}H HSQC spectra of the free enzyme recorded in the range pH 4–7 (data not shown) the α-amino group remains invisible implying that it is not hydrogen bonded. Furthermore, as shown in Table II, the ^{15}N and ^{1}H chemical shifts of the backbone amide groups of residues one to four do not change appreciably in the pH range 4.3–6.9 while their resonances shift upfield (corresponding to α-helix formation) in the presence of micelles and inhibitor. Thus, pH differences do not explain the structural differences in the N-terminal region between crystal and solution structures. They may actually arise from inter-molecular contacts in the crystal, since several contacts are observed involving the side chain of Trp3 of porcine PLA_2 (Dijkstra *et al.*, 1983; Finzel *et al.*, 1991).

In Figure 4 three selected segments of PLA_2 are shown. In Figure 4A several side chain–side chain contacts between helix A and the large β-sheet are indicated. The position of the tip of the sheet is well-defined because of the presence of multiple interactions between Ala12 and Pro14 at the end of helix A, and Asn79, Thr80 and Ile82

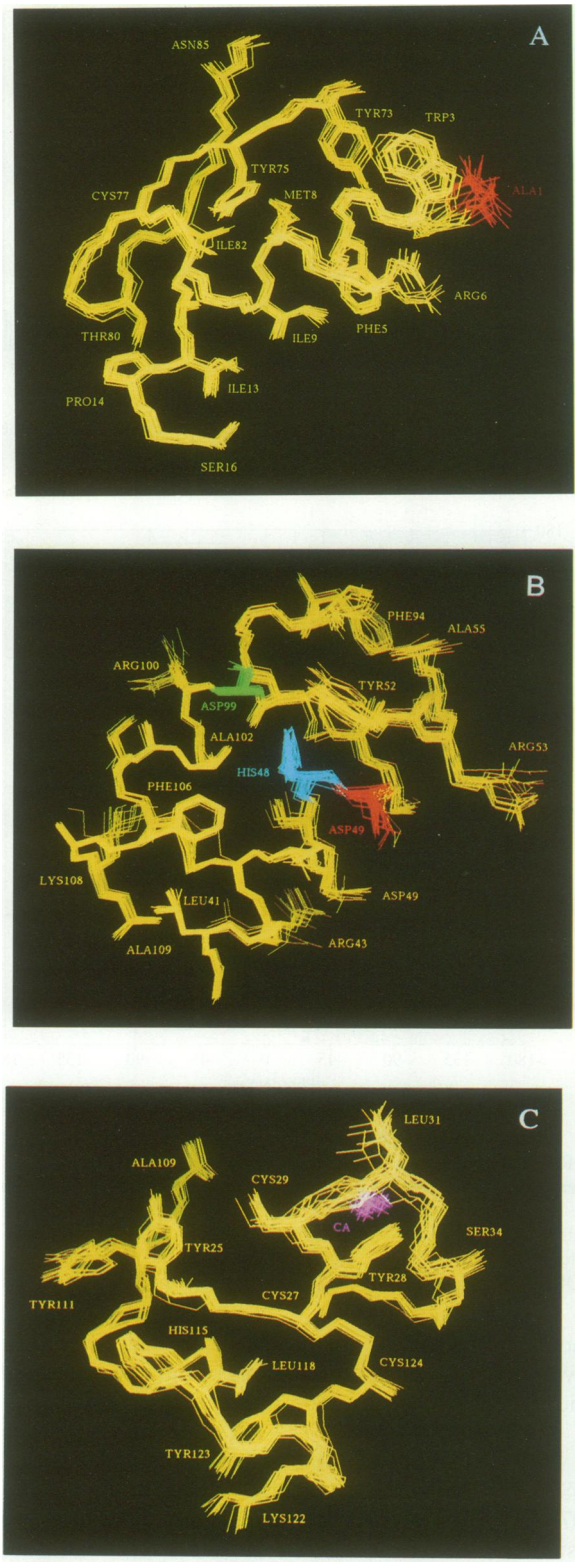

Fig. 4. Best-fit superpositions of all atoms (excluding hydrogens and backbone carbonyls) of the 20 refined distance geometry structures for three selected segments of PLA_2. Side chain–side chain contacts between helix A and the β-sheet are shown in (**A**), contacts between the central helices C and D are shown in (**B**) and in (**C**) contacts between the C-terminal part of PLA_2 and the calcium loop are presented. For clarity not all amino acid residues are shown. In (A) the residue Ala1 is shown in red. In (B) the active site residues His48, Asp99 and Asp49 are shown in blue, green and red, respectively. In (C) the calcium ion is indicated in purple.

in the tip of the β-sheet. The positions of helix A and the β-sheet are further determined by numerous contacts between the side chains of Met8, Cys11, Tyr75 and Ile82. Further inspection of Figure 4A once more reveals the disordered structure of residues Ala1, Leu2 and Trp3.

The central core of PLA_2 consists mainly of the two large, antiparallel running α-helices C and D, which are indicated in Figure 4B. The positions of most side chains are well-defined due to the presence of many long range NOEs between residues in both helices. These contacts involve the residues Leu41, Cys44, the active site His48, Tyr52, Ala55 and Leu58 in helix C, and the residues Phe94, Ile95, the active site Asp99, Ala102, Phe106 and Ala109 in helix D. In contrast, several side chains of solvent exposed residues are poorly defined, among them Arg100, Arg53, Arg43 and Asp49.

The last segment of PLA_2 shown in Figure 4 is the C-terminal part of the protein, which is linked to the calcium binding loop via the disulfide bridge between residues 27 and 124 (Figure 4C). With the exception of Tyr111 and the side chains of the solvent exposed residues Asn112, Lys113, Glu114, Lys116 and Lys121, this part of the protein is also well-defined. The position of the calcium binding loop is constrained by several long range interactions present between Gly35 and Cys124, Cys29 and Cys45, and Cys27 and Thr120. In addition, many contacts are present between the aromatic ring of Tyr28 and other residues in the calcium binding loop. The resonances in the C-terminal part of PLA_2 (starting at residue 114) show in general very intense correlations in the HCCH-TOCSY spectra, which could point to some mobility in this part of the protein.

The differences between the NMR and X-ray structures

In Figure 5A the superposition of the α-carbons of the PLA_2 is shown for the restrained average minimized NMR structure and the X-ray structure of Finzel *et al.* (1991). The differences in the α-carbon positions as a function of the residue number are also shown (Figure 5B). It is clear that the NMR and X-ray structure are very similar in secondary structure, but significant differences are present in tertiary structure. Excluding residues 59–72 in the highly flexible surface loop, the r.m.s. difference between the restrained minimized NMR structure and the X-ray structure is 2.5 Å for the backbone atoms and 3.4 Å for all atoms. These differences are large compared with the r.m.s. differences of 0.6 Å for the backbone atoms and 1.1 Å for all atoms between the two crystal structures of porcine pancreatic PLA_2 (Dijkstra *et al.*, 1983; Finzel *et al.*, 1991). A close inspection of Figure 5B shows that the α-helices are fairly well superimposable, with deviations in α-carbon positions of 1.6 Å. Large structural differences are mainly found in loops connecting the secondary structure elements like loop 14–17 connecting helix A to helix B, the calcium binding loop (residues 28–34), the surface loop (residues 59–72) and loop 85–88 connecting the β-sheet to helix D. Other large differences between the NMR and X-ray structures occur in the tip of the β-sheet and in the C-terminal region (residues 119–124). Part of the differences in the surface loops in the NMR and X-ray structures may be ascribed to differences in protonation under the experimental conditions. This is

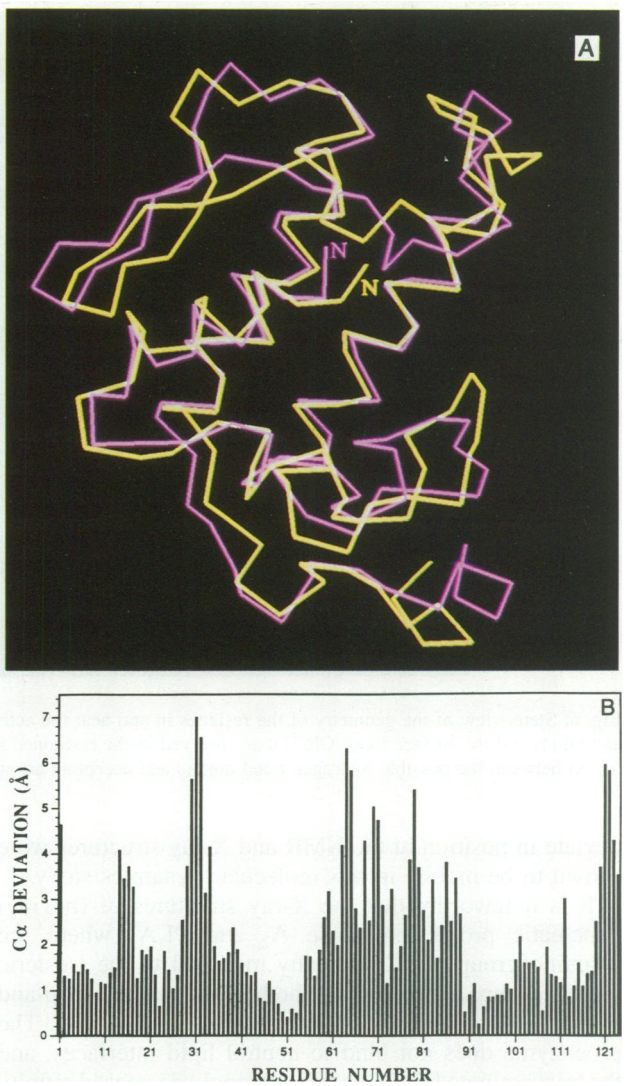

Fig. 5. Best-fit superposition of the Cα atoms of the restrained minimized averaged NMR structure (shown in yellow) and the X-ray structure (shown in purple) of PLA_2 (**A**). Deviations that occur in α-carbon positions between the restrained minimized averaged NMR structure and the X-ray structure, shown as a function of the residue number (**B**). The crystal structure is that of Finzel *et al.* (1991).

especially true for loops 14–17 (with His17), for the calcium binding loop, for loop 59–72 (with Asp59, Asp66 and Glu71) and for the C-terminal region (with Glu114, His115 and Asp119). Other differences are probably due to different mobilities that are possible in solution and in crystals where protein–protein contacts may play a role. In the crystal structure of porcine pancreatic phospholipase A_2 (Dijkstra *et al.*, 1983) a second calcium ion (different from the 'catalytic' one) is shared by two PLA_2 molecules and the ion is coordinated by Ser72 and Glu92 of both monomers. The differences in the surface–exposed loop connecting helices A and B and in the loop connecting the β-sheet with helix D are probably caused by mobility in solution and crystal packing. Furthermore, it is interesting to note that time-averaged restrained molecular dynamics refinement of the X-ray structure indicates that the calcium binding loop and the surface loop are very mobile (Gros *et al.*, 1990). In addition, all regions that

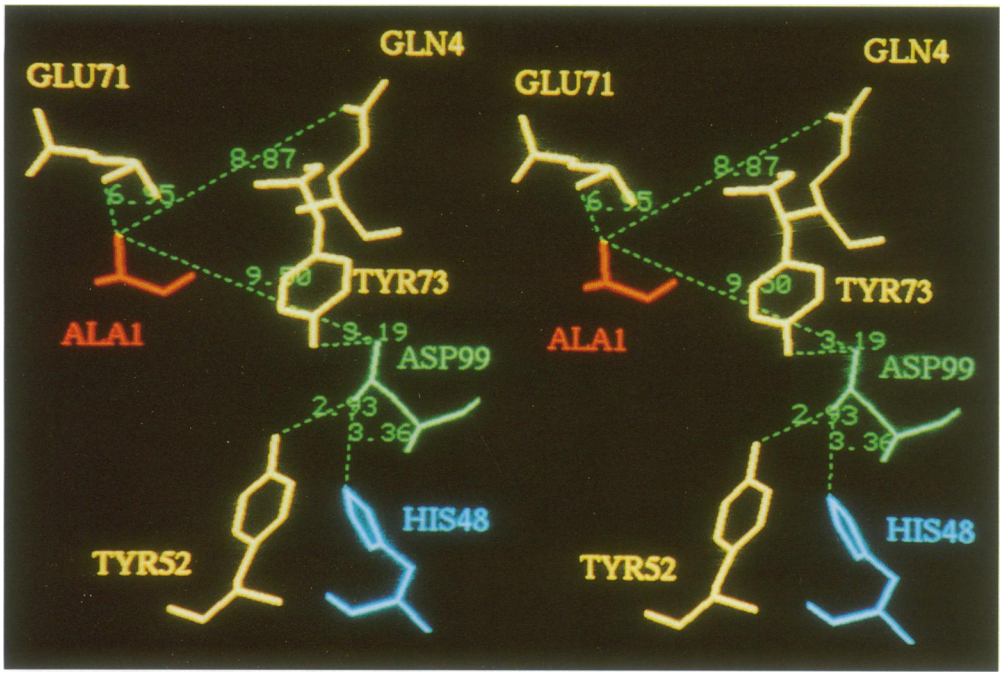

Fig. 6. Stereoview of the geometry of the residues in and near the active site (His48, Tyr52, Tyr73 and Asp99) and residues in the N-terminus (Ala1 and Gln4) and the surface loop (Glu71), as observed in the restrained minimized averaged NMR structure of PLA_2 free in solution. The distances (in Å) between the possible hydrogen bond donors and acceptors are indicated in green.

deviate in position in the NMR and X-ray structures were shown to be mobile in this molecular dynamics study.

It is noteworthy that the X-ray structures of (bovine) pancreatic prophospholipase A_2 and PLA_2 where the α-amino group was chemically modified to the isosteric α-keto group, are disordered both in the surface loop and in the N-terminal helix (Dijkstra *et al.*, 1982, 1984). The proenzyme does not bind to neutral lipid interfaces, and the transaminated PLA_2 shows a strongly decreased affinity towards zwitterionic lipid interfaces, in combination with a total loss of activity on micellar substrates (Verheij *et al.*, 1981). Both the prophospholipase A_2 and the transaminated PLA_2 readily bind to negatively charged interfaces, but no enzymatic activity is observed (Maliwal *et al.*, 1994). Thus the structure that we observe for mature PLA_2 in the absence of interfaces strongly resembles the X-ray structure of the inactive, highly homologous, bovine α-keto PLA_2 and $proPLA_2$.

Significance of the NMR structure for the mechanism of interfacial activation

Lipolytic enzymes are characterized by interfacial activation: the catalytic activities of these enzymes are very low on monomeric substrates, whereas on aggregated substrates the activities increase dramatically. The mechanism behind this activation process is a long-standing problem. For several lipases, X-ray crystallographic studies have indicated that enzymatic conformational changes are important in the activation process. For instance, in the case of the lipase from *Rhizomucor miehei* it was concluded that upon interaction with a lipid interface a large hydrophobic surface becomes exposed (Tilbeurgh *et al.*, 1993). In contrast, for PLA_2s the extensive crystallographic data suggest a structurally invariant enzyme. Rather a facilitated diffusion of substrates into a rigid dehydrated active site is so far held responsible for the high catalytic activities of PLA_2s on aggregated substrates. The present study, however, sheds a different light on the mechanism of interfacial activation of the latter enzyme.

In Figure 6 the region of the active site residues and the residues involved in the hydrogen bonding network are shown, as present in the restrained minimized averaged NMR structure. The active site in our NMR structure resembles the geometry of the active site found in the X-ray structures. The hydrogen bonds which are present in the X-ray structures between Tyr52, Tyr73 and Asp99, and the hydrogen bond between the active site residues His48 and Asp99, are also possible in the NMR structure. On the other hand, the Ala1 α-amino group and both the side chain carbonyl of Gln4 and the backbone carbonyl of Glu71, which are part of the hydrogen bonding network in the X-ray structure, are more than 7 Å apart in the solution structure. In addition, the distances of the α-amino group to the active center residues Asp99 and Tyr52 are more than 9 Å, which is too large even to form a water-mediated hydrogen bond. In the crystal structures of porcine pancreatic PLA_2 the distances between the α-amino group and the active site residues are ~6 Å, and water-mediated hydrogen bonds are supposed to be present (Dijkstra *et al.*, 1983; Finzel *et al.*, 1991). Thus, the NMR structures indicate that in free PLA_2, as in the X-ray structure of $proPLA_2$, only a part of the hydrogen bonding network is present. The absence of hydrogen bonds between the α-amino group and the active site might render the active site residues conformational freedom, which could be related to the low catalytic activities of free PLA_2 on monomeric substrates. If the first three N-terminal residues are present in an α-helical conformation with the α-amino group occupying a position closer to the active site, as is seen in the crystal structures, this

could lead to a rigid, highly active conformation of the active site residues. We propose that when PLA_2 binds to a lipid interface and subsequently binds a substrate or inhibitor in the active site, this α-helical conformation of the N-terminus is induced. Indeed, recent NMR studies suggest that an ordered N-terminal structure is present in PLA_2 bound to lipid micelles, with a competitive inhibitor present in the active site (Peters *et al.*, 1992; van den Berg *et al.*, 1995).

In conclusion, we have determined the high-resolution structure of free porcine pancreatic PLA_2 by NMR. The solution structure deviates from the crystal structure in several regions of the protein. The most important differences are found in the N-terminal region, and in a surface loop (59–72), which are disordered in solution and in proPLA_2, whereas in the crystal structure of the mature PLA_2 a well-defined α-helical conformation is present. In the NMR structure the hydrogen bonding network linking the N-terminal α-amino group to the active site is incomplete. Biochemical data indicate that a fixed conformation of the α-amino group is essential for binding of the enzyme to lipid–water interfaces and catalytic activity (Verheij *et al.*, 1981). We propose that the observed flexibility in solution of the N-terminal region, loop 59–72 and the active site residues result in low catalytic activities. We also propose that when the enzyme complexes to a lipid–water interface and binds a substrate or inhibitor molecule in the active site, these residues adopt an optimal, rigid conformation, leading to high catalytic activities. Experimental evidence for the induction of an ordered structure of PLA_2 in such a complex has already been obtained (Peters *et al.*, 1992; van den Berg *et al.*, 1995). The observation of a rigid, N-terminal α-helix in the crystal structures of free PLA_2 might be the result of a preferential crystallization of the protein conformer resembling the enzyme complexed to lipids. In summary, the solution structure of PLA_2 suggests that enzymatic conformational changes are involved in the mechanism of interfacial activation not only for lipases, but also for PLA_2.

Materials and methods

Sample preparation

Uniformly (>90%) ^{15}N,^{13}C-labeled porcine pancreatic PLA_2 was expressed in *Escherichia coli* using a derivative of the expression vector pGEX-T2 (Pharmacia, Sweden). This derivative was obtained from the pGEX-T2 expression vector by deletion of the *Msc*I–*Bam*HI fragment after filling in *Bam*HI, and is denoted pAB_3. The *Bam*HI–*Hin*dIII fragment encoding wild type PLA_2 (Kuipers *et al.*, 1989) was cloned into the similarly cut expression vector pAB_3. The resulting 21 kDa fusion protein contains the PLA_2 moiety fused via a small linker to the N-terminal 70 amino acids of the glutathione S-transferase of *Schistosoma japonicum*, which is under control of the IPTG-inducible *tac* promoter (Smith and Johnson, 1988). The *E.coli* strain BL21 (de3) was used for expression of the fusion protein. The labeled protein was prepared in 2.5 l of synthetic medium, consisting of 4.4 g KH_2PO_4, 7.8 g K_2HPO_4, 1 g NH_4Cl, 10 mg $(NH_4)_2Fe(SO_4)_3$ and 50 mg $MgSO_4.7H_2O$ per liter. Glucose was added to 2 g/l, thiamine was added to a concentration of 10 mg/l, and ampicillin to 100 mg/l. For labeling uniformly labeled ^{15}N-labeled NH_4Cl and [$^{13}C6$]glucose was used (Cambridge Isotope Laboratories). The fermenter was kept at 37°C, with stirring at 400 r.p.m. and vigorous aeration. After 3 h of growth PLA_2 production was induced by adding IPTG to a final concentration of 0.4 mM and an additional amount of ampicillin to 50 mg/l. Cells were harvested after another 4 h of growth, and centrifuged. The isolation of inclusion bodies and sulfonation of the fusion protein were done as described earlier (de Geus, 1986). Reoxidation of the protein was performed in a mixture containing 2 M urea, 5 mM EDTA, 8 mM cysteine, 1 mM cystine and 10 mM borate at pH 8.8. The refolding took place at room temperature, in the dark, for a period of 20 h. The PLA_2 concentration in the refolding buffer was ~50 mg/l. After refolding, the PLA_2 moiety was liberated from the pAB_3 fusion protein by mild trypsinolysis at pH 8.2 in the presence of 5 mM calcium. The PLA_2 was purified to homogeneity using two subsequent CM-cellulose ion exchange columns (CM-52, Whatman) at pH 4.8 and 5.8, respectively. PLA_2 activity was routinely determined in the egg-yolk assay (Nieuwenhuizen *et al.*, 1974). The obtained yield was 32 mg of pure doubly labeled PLA_2. The samples for NMR spectroscopy contained typically 2.5 mM protein at pH 4.3, dissolved in either 99.96% D_2O or 93% H_2O/7% D_2O, with 50 mM $CaCl_2$ and 150 mM NaCl. The ^{15}N-^1H HSQC pH titration experiment was performed at pH values of 4.3, 4.9, 5.6 and 6.9 with a 0.45 mM protein sample containing the same salts.

NMR spectroscopy

All 3D NMR spectra were recorded at 313 K on a Bruker AMX600 spectrometer equipped with a three channel NMR interface and a triple-resonance ^1H,^{15}N,^{13}C probe with an additional gradient coil. Some 2D HMQC and HSQC experiments were recorded on a Bruker AMX500 spectrometer. A set of four triple-resonance ^1H,^{15}N,^{13}C experiments was recorded to obtain the backbone sequential assignments, consisting of HNCA, HNCO, HN(CO)CA and HCACO spectra (Ikura *et al.*, 1990a; Kay *et al.*,1990; Bax and Ikura, 1991). The assignment of side chain proton and carbon resonances was carried out using double resonance ^1H,^{13}C 3D HC(C)H-COSY (Bax *et al.*, 1990b), several 3D HCCH-TOCSY (Bax *et al.*, 1990a,b) and ^{15}N-edited TOCSY-HSQC spectra (Marion *et al.*, 1989a). The assignment of the NOEs was obtained using one 3D ^{15}N-edited NOESY-HSQC (Marion *et al.*, 1989a) and two 3D ^{13}C-edited NOESY-HSQC (Ikura *et al.*, 1990b) experiments. The HCACO, HCCH-COSY, HCCH-TOCSY and ^{13}C-edited NOESY experiments were recorded in D_2O, while all other spectra were recorded in 93% H_2O/7% D_2O. Water suppression was achieved by presaturation during the recovery delay for the HNCA, HNCO and HNCOCA experiments. In the case of the ^{15}N-edited NOESY-HSQC experiment, water suppression was improved by the use of pulsed field gradients and trim pulses to randomize magnetization of protons not attached to ^{15}N. Quadrature detection in the indirectly detected dimensions was achieved using the TPPI method (Marion and Wüthrich, 1983) for the HNCA, HNCO, HN(CO)CA and HCACO experiments, and the States-TPPI method (Marion *et al.*, 1989b) for all other experiments. In Table II the NMR experiments which were used in the present study are listed, together with the spectral parameters. All NMR spectra were processed on Silicon Graphics workstations using the TRITON software package; one or two times zero-filling was employed in all indirectly detected dimensions. Linear prediction was in most cases used to extend the data by ~30% in the heteronuclear dimensions. Separate baseline corrections were applied after the Fourier transformations and appropriate window function multiplications. The spectra were analysed directly on a Silicon Graphics workstation using the program ALISON.

Assignment strategy

Previously, ~90% of the ^1H and ^{15}N resonances of PLA_2 had been assigned using ^{15}N-labeled PLA_2 and analyzing ^{15}N-edited NOESY-HSQC and TOCSY-HSQC spectra (Dekker *et al.*, 1991). However, the relatively high α-helical content (~50% according to the X-ray structures) of PLA_2 causes a limited dispersion of the resonances in the ^1H and ^{15}N dimensions. The limited spectral regions, together with the relatively broad resonance lines in the spectra, makes the conventional sequential assignment procedure (Wüthrich , 1986) rather difficult for PLA_2. For this reason we reassigned the backbone resonances of PLA_2 by a strategy of using triple-resonance spectra in combination with a conventional ^{15}N-edited TOCSY spectrum (Grzesiek *et al.*, 1992). With the backbone assignments as a starting point, the amino acid side chains were assigned by analyzing the HCCH-COSY and HCCH-TOCSY experiments. The stereospecific assignments for all prochiral methyl groups of leucine and valine residues were obtained from a ^1H-^{13}C HMQC spectrum recorded on a sample of 10% ^{13}C-labeled PLA_2 (Senn *et al.*, 1989). In the present study, no stereospecific assignments for prochiral non-degenerate (β, γ, δ, ε) methylene protons and glycine α-protons were used.

Constraints

NOEs were assigned from 2D ^1H-^1H NOESY and from 3D ^{13}C- and ^{15}N-edited NOESY spectra, recorded with mixing times ranging from 100 to 150 ms. NOEs were classified as strong, medium, weak and very

weak, corresponding to interproton distance constraints of 2.0–2.8 Å, 2.0–3.7 Å, 2.0–5.0 Å and 2.0–5.5 Å respectively. For the upper distance limits for NOE distances involving methyl protons, non-stereospecifically assigned methylene protons and aromatic ring protons, pseudo atom corrections were applied of 1.0, 0.9 and 2.0 Å respectively. Qualitative constraints for ϕ torsion angles were obtained from a ^{15}N HMQC-J experiment (Kay and Bax, 1989). For $^{3}J_{HN\alpha} < 6$ Hz, ϕ was constrained to $-50 \pm 40°$; for $^{3}J_{HN\alpha} > 4$ Hz, ϕ was constrained to $-125 \pm 50°$ (Pardi *et al.*, 1984). In the present study no ψ and $\chi 1$ torsion angle constraints were used. Because of problems associated with the correct assignment of hydrogen bonds based on slowly exchanging amide protons and NOE data, hydrogen bond constraints were not introduced. Constraints for the calcium ion were not used in the determination of the distance geometry structures. However, because the calcium binding loop tended to drift away in the refinement procedure, five distances derived from the X-ray structures were used to constrain a neutral calcium 'ion' during refinement. These distances, involving both carboxyl oxygens of Asp49 and the three backbone carbonyl oxygens of Tyr28, Gly30 and Gly32, were constrained from 3.0 to 4.0 Å.

Structure calculations

Protein structures were generated with distance geometry (Havel, 1991) using the DGII program (Biosym, San Diego, CA). The structures were refined with the program Discover (Biosym). The refinement protocol consisted of a restrained Energy Minimization step (100 iterations using steepest descents minimization followed by 1000 iterations using conjugate gradients minimization), followed by restrained Molecular Dynamics for 6 ps, using a Consistent Valence Forcefield (CVFF). Finally, another Energy Minimization step was performed (250 steepest descent steps followed by 2000 conjugate gradients steps). Displaying and visual inspection of the structures was performed on Silicon Graphics workstations, using the InsightII program implemented in the NMRchitect software package (Biosym).

Iterative structure refinement

The initial structures, determined on the basis of ~1000 approximate distance constraints, had a precision which was already sufficient to solve many ambiguities in the assignment of NOEs from the ^{13}C-edited NOESY spectra, as these spectra still show considerable overlap in the most crowded regions. Furthermore, the structures also aided in the identification of several wrongly assigned NOEs. The final structures were calculated by using an iterative structure refinement as described in the literature (Powers *et al.*, 1993). The final constraint list consisted of a total of 1824 experimental constraints, comprising 1727 approximate interproton distance constraints which could be subdivided in the following way: 349 intra-residue, 472 sequential ($|i-j| = 1$), 357 medium-range ($2 \leq |i-j| \leq 5$) and 549 long range ($|i-j| > 5$) constraints. Furthermore, 97 constraints for dihedral ϕ torsion angles were obtained from the ^{15}N HMQC-J spectrum.

The atomic coordinates of the NMR structure of porcine pancreatic PLA_2, together with the constraints and the chemical shifts have been deposited in the Brookhaven protein databank.

References

Bax,A., Clore,G.M., Driscoll,P.C., Gronenborn,A.M., Ikura,M. and Kay,L.E. (1990a) Practical aspects of proton-carbon-carbon-proton three-dimensional correlation spectroscopy of ^{13}C-enriched proteins. *J. Magn. Resonance*, **87**, 620–627.

Bax,A., Clore,G.M. and Gronenborn,A.M. (1990b) ^{1}H-^{1}H correlation via isotropic mixing of magnetization, a new three-dimensional approach for assigning ^{1}H and ^{13}C spectra of ^{13}C-enriched proteins. *J. Magn. Resonance*, **88**, 425–431.

Bax,A.and Ikura,M. (1991) An efficient 3D NMR technique for correlating the proton and ^{15}N backbone amide resonances with the α-carbon of the preceding residue in uniformly ^{15}N/^{13}C enriched proteins. *J. Biomol. NMR*, **1**, 99–104.

Brady,L. *et al.* (1990) A serine protease triad forms the catalytic centre of a triacylglycerol lipase. *Nature*, **343**, 767–770.

Brunie,S., Bolin,J., Gewirth,D. and Sigler,P.B. (1985) The refined crystal structure of dimeric phospholipase A_2 at 2.5 Å. *J. Biol. Chem.*, **260**, 9742–9749.

Brzozowski,A.M. *et al.* (1991) A model for interfacial activation in lipases from the structure of a fungal lipase-inhibitor complex. *Nature*, **351**, 491–494.

Clore,G.M. and Gronenborn,A.M. (1991) Structures of larger proteins in solution: three- and four-dimensional heteronuclear NMR spectroscopy. *Science*, **252**, 1390–1399.

Clore,G.M., Robien,M.A. and Gronenborn, A.M. (1993) Exploring the limits of precision and accuracy of protein structures determined by nuclear magnetic resonance spectroscopy. *J. Mol. Biol.*, **231**, 82–102.

De Geus, P. (1986) Application of Recombinant DNA Techniques in the Study of Phospholipases A. Ph.D. Thesis, University of Utrecht, Utrecht, the Netherlands.

Dekker,N., Peters,A.R., Slotboom,A.J., Boelens,R., Kaptein,R. and Haas,G.H. de (1991) Porcine pancreatic phospholipase A_2: sequence-specific ^{1}H and ^{15}N NMR assignments and secondary structure. *Biochemistry*, **30**, 3135–3147.

Demaret,J.-P. and Brunie,S. (1990) Molecular dynamics simulations of phospholipases A_2. *Protein Engng*, **4**, 163–170.

Dijkstra,B.W., Kalk,K.H., Hol,W.G.J. and Drenth,J. (1981) Structure of bovine pancreatic phospholipase A_2 at 1.7 Å resolution. *J. Mol. Biol.*, **147**, 97–123.

Dijkstra,B.W., van Nes,G.J.H., Kalk,K.H., Brandenburg,N.P., Hol,W.G.J. and Drenth,J. (1982) The structure of bovine prophospholipase A_2 at 3.0 Å resolution. *Acta Crystallogr.*, **B38**, 793–799.

Dijkstra,B.W., Renetseder,R. Kalk,K.H., Hol,W.G.J. and Drenth,J. (1983) Structure of porcine pancreatic phospholipase A_2 at 2.6 Å resolution and comparison with bovine phospholipase A_2. *J. Mol. Biol.*, **168**, 163–179.

Dijkstra,B.W., Kalk,K.H., Drenth,J., de Haas,G.H., Egmond,M.R. and Slotboom,A.J. (1984) Role of the N-terminus in the interaction of pancreatic phospholipase A_2 with aggregated substrates. Properties and crystal structure of transaminated phospholipase A_2. *Biochemistry*, **23**, 2759–2766.

Finzel,B.C., Ohlendorf,D.H., Weber,P.C. and Salemme,F.R. (1991) An independent crystallographic refinement of porcine pancreatic phospholipase A_2 at 2.4 Å resolution. *Acta Crystallogr.*, **B47**, 558–559.

Fisher,J., Roberts,G.C.K., Dekker,N., Boelens,R., Kaptein,R. and Slotboom,A.J. (1989) ^{1}H NMR studies of bovine and porcine phospholipase A_2: assignment of aromatic residues and evidence for conformational equilibrium in solution. *Biochemistry*, **28**, 5939–5946.

Gros,P., van Gunsteren,W.F. and Hol,W.G.J. (1990) Inclusion of thermal motion in crystallographic structures by restrained molecular dynamics. *Science*, **249**, 1149–1152.

Grzesiek,S., Döbeli,H., Gentz,R., Garotta,G., Labhardt,A.M. and Bax,A. (1992) ^{1}H, ^{13}C and ^{15}N NMR backbone assignments and secondary structure of human interferon-γ. *Biochemistry*, **31**, 8180–8190.

Havel,T.F. (1991) An evaluation of computational strategies for use in the determination of protein structure from distance constraints obtained by nuclear magnetic resonance. *Prog. Biophys. Mol. Biol.*, **56**, 43–78.

Ikura,M., Kay,L.E. and Bax,A. (1990a) A novel approach for sequential assignment of ^{1}H, ^{13}C, and ^{15}N spectra of larger proteins: heteronuclear triple-resonance three-dimensional NMR spectroscopy. *Biochemistry*, **29**, 4659–4667.

Ikura,M., Kay,L.E., Tschudin,R. and Bax,A. (1990b) Three-dimensional NOESY-HMQC spectroscopy of a ^{13}C-labeled protein. *J. Magn. Resonance*, **86**, 204–209.

Kay,L.E. and Bax,A. (1989) New methods for the measurement of NH-CαH coupling constants in ^{15}N-labeled proteins. *J. Magn. Resonance*, **86**, 110–126.

Kay,L.E., Ikura,M., Tschudin,R. and Bax,A. (1990) Three-dimensional triple-resonance NMR spectroscopy of isotopically enriched proteins. *J. Magn. Res.*, **89**, 496–514.

Kuipers,O.P., Thunnissen,M.M.G.M., Geus,P.de, Dijkstra,B.W., Drenth,J., Verheij,H.M. and de Haas,G.H. (1989) Enhanced activity and altered specificity of phospholipase A_2 by deletion of a surface loop. *Science*, **244**, 82–85.

Maliwal,B.P., Yu,B.-Z., Szmacinski,H., Squier,T., Van Binsbergen,J., Slotboot,A.J.,and Jain,M.K. (1994) Functional significance of the conformational dynamics of the N-terminal segment of secreted phospholipase A_2 at the interface. *Biochemistry*, **33**, 4509–4516.

Marion,D. and Wüthrich,K. (1983) Application of phase-sensitive two-dimensional correlated spectroscopy (COSY) for measurements of ^{1}H-^{1}H spin-spin coupling constants in proteins. *Biochem. Biophys. Res. Commun.*, **113**, 967–974.

Marion,D., Driscoll,P.C., Kay,L.E., Wingfiels,P.T., Bax,A., Gronenborn, A.M. and Clore,G.M. (1989a) Overcoming the overlap problem in the assignment of ^{1}H NMR spectra of larger proteins by use of three-dimensional heteronuclear ^{1}H-^{15}N Hartmann-Hahn-multiple quantum coherence and Nuclear Overhauser-multiple quantum coherence spectroscopy: application to interleukin 1β. *Biochemistry*, **28**, 6150–6156.

Marion,D., Ikura,M., Tschudin,R. and Bax,A. (1989b) Rapid recording of 2D NMR spectra without phase cycling. Application to the study of hydrogen exchange in proteins. *J. Magn. Resonance*, **85**, 393–399.

Morris,A.L., MacArthur,W.M., Hutchinson,E.G. and Thornton,J.M. (1992) Stereochemical quality of protein structure coordinates. *Proteins*, **12**, 345–364.

Nieuwenhuizen,W., Kunze,H. and de Haas,G.H. (1974) Phospholipase A_2 (phosphatide acylhydrolase, EC 3.1.1.4) from porcine pancreas. *Methods Enzymol.*, **32 B**, 147–154.

Pardi,A., Billeter,M. and Wüthrich,K. (1984) Calibration of the angular dependence of the amide proton-C^{α} proton coupling constants, $^3J_{HN\alpha}$, in a globular protein. *J. Mol. Biol.*, **180**, 741–747.

Peters,A.R., Dekker,N., van den Berg,L., Boelens,R., Kaptein,R., Slotboom,A. and de Haas,G.H. (1992) Conformational changes in phospholipase A_2 upon binding to micellar interfaces in the absence and presence of competitive inhibitors. A ^1H and ^{15}N NMR study. *Biochemistry*, **31**, 10024–10030.

Powers,R., Garrett,D.S., March,C.J., Frieden,E.A., Gronenborn,A.M. and Clore,G.M. (1993) The high-resolution, three-dimensional solution structure of human interleukin-4 determined by multidimensional heteronuclear magnetic resonance spectroscopy. *Biochemistry*, **32**, 6744–6762.

Renetseder,R., Brunie,S., Dijkstra,B.W., Drenth,J. and Sigler,P.B. (1985) A comparison of the crystal structures of phospholipase A2 from bovine pancreas and *Crotalus atrox* snake venom. *J. Biol. Chem.*, **260**, 11627–11634.

Scott,D.L., White,S.P., Otwinowski,Z., Yuan,W., Gelb,M.H. and Sigler,P.B. (1990) Interfacial catalysis: the mechanism of phospholipase A_2. *Science*, **250**, 1541- 1546.

Scott,D.L., White,S.P., Browning,J.L., Rosa,J.J., Gelb,M.H. and Sigler,P.B. (1991) Structures of free and inhibited human secretory phospholipase A_2 from inflammatory exudate. *Science*, **254**, 1007–1010.

Scott,D.L. and Sigler,P.B. (1994) Structure and catalytic mechanism of secretory phospholipases A_2. *Adv. Protein Chem.*, **45**, 53–88.

Senn,H., Werner,B., Messerle,B.A., Weber,C., Traber,R. and Wüthrich,K. (1989) Stereospecific assignment of the methyl ^1H NMR lines of valine and leucine in polypeptides by nonrandom ^{13}C labelling. *FEBS Lett.*, **249**, 113–118.

Smith,B.S. and Johnson,K.S. (1988) Single-step purification of polypeptides expressed in *Escherichia coli* as fusions with glutathione S-transferase. *Gene*, **67**, 31–40.

Thunnissen,M.M.G.M. Ab,E., Kalk,K.H., Drenth,J., Dijkstra,B.W., Kuipers,O.P., Dijkman,R., de Haas,G.H. and Verheij,H.M. (1990) X-ray structure of phospholipase A_2 complexed with a substrate-derived inhibitor. *Nature*, **347**, 689–691.

Tilbeurgh,H. van, Egloff,M-P, Martinez,C., Rugani,N., Verger,R. and Cambillau,C. (1993) Interfacial activation of the lipase-procolipase complex by mixed micelles revealed by X-ray crystallography. *Nature*, **362**, 814–820.

Tomoo,K. Ohishi,H., Doi,M., Ishida,T., Inoue,M., Ikeda,K. and Mizuno,H. (1992) Interaction mode of *n*-dodecylphosphoryl-choline, a substrate analogue, with bovine pancreas phospholipase A_2 as determined by X-ray crystal analysis. *Biochem. Biophys. Res. Commun.*, **187**, 821–827.

Van den Berg,B., Tessari,M., Boelens,R., Dijkman,R., Kaptein,R., de Haas,G.H. and Verheij,H.M. (1995) Solution structure of porcine pancreatic phospholipase A_2 complexed with micelles and a competitive inhibitor. *J. Biomol. NMR*, **5**, 110–121

Verger,R. and de Haas,G.H. (1976) Interfacial enzyme kinetics of lipolysis. *Annu. Rev. Biophys. Bioengng*, **5**, 77–117.

Verheij,H.M., Volwerk,J.J., Jansen,E.H.J.M., Puyk,W.C., Dijkstra,B.W., Drenth,J. and de Haas,G.H. (1980) Methylation of histidine-48 in pancreatic phospholipase A_2. Role of histidine and calcium ion in the catalytic mechanism. *Biochemistry*, **19**, 43–50.

Verheij,H.M., Egmond,M.R. and Haas,G.H. de (1981) Chemical modification of the α-amino group in snake venom phospholipases A_2. *Biochemistry*, **20**, 9499.

Volwerk,J.J. and de Haas,G.H. (1982) In Griffith,O.H. and Jost,P.C. (eds), *Molecular Biology of Lipid-Protein Interactions*. Wiley, New York, pp.69–150.

Waite,M. (1987) The phospholipases. In Hanahan,D.J., (ed.), *Handbook of Lipid Research Vol. 5*. Plenum Press, New York.

Wery,J.P. *et al.* (1991) Structure of recombinant human rheumatoid arthritic synovial fluid phospholipase A_2 at 2.2 Å resolution. *Nature*, **352**, 79–82.

Westerlund,B., Nordlund,P., Uhlin,U., Eaker,D. and Eklund,H. (1992) The three-dimensional structure of notexin, a presynaptic neurotoxic phospholipase A_2 at 2.0 Å resolution. *FEBS*, **10928**, 159–164.

White,S.P., Scott,D.L., Otwinowski,Z., Gelb,M.H. and Sigler,P.B. (1990) Crystal structure of cobra-venom phospholipase A_2 in a complex with a transition-state analogue. *Science*, **250**, 1560–1563.

Wüthrich,K. (1986) *NMR of Proteins and Nucleic Acids*. John Wiley & Sons Inc., New York.

Received on March 21, 1995; revised on April 28, 1995